

1 **Distribution of *Alexandrium fundyense* (dinophyceae) cysts in Greenland and**
2 **Iceland, with an emphasis on viability and growth in the Arctic**

3

4 Mindy L. Richlen^{1*}, Oliver Zielinski², Lars Holinde², Urban Tillmann³, Allan
5 Cembella³, Yihua Lyu^{1,4}, Donald M. Anderson¹

6

7 ¹ Woods Hole Oceanographic Institution, 266 Woods Hole Rd., MS 32, Woods Hole,
8 Massachusetts 02543, USA

9 ² Institute for Chemistry and Biology of the Marine Environment, University of
10 Oldenburg, 26111 Oldenburg, Germany

11 ³ Alfred-Wegener-Institut, Helmholtz Zentrum für Polar-und Meeresforschung, Am
12 Handelshafen 12, 27570 Bremerhaven, Germany

13 ⁴ State Key Lab of Marine Environmental Science, School of Life Science, Xiamen
14 University, Xiamen, 361102, China

15

16

17

18 *Corresponding author E-mail: mrichlen@whoi.edu

19

20 **Running page head: *Alexandrium fundyense* cysts in Arctic waters**

21

22 **Key words:** Arctic, *Alexandrium*, dinoflagellate, cysts, harmful algal bloom

23

24 **ABSTRACT**

25 The bloom-forming dinoflagellate *Alexandrium fundyense* has been
26 extensively studied due its toxin-producing capabilities and consequent impacts to
27 human health and economies. This study investigated the prevalence of resting cysts
28 of *A. fundyense* in western Greenland and Iceland to assess the historical presence and
29 magnitude of bloom populations in the region, and to characterize environmental
30 conditions during summer, when bloom development may occur. Analysis of
31 sediments collected from these locations showed that *Alexandrium* cysts were present
32 at low to moderate densities in most areas surveyed, with highest densities observed
33 in western Iceland. Additionally, laboratory experiments were conducted on clonal
34 cultures established from isolated cysts or vegetative cells from Greenland, Iceland,
35 and the Chukchi Sea (near Alaska) to examine the effects of photoperiod interval and
36 irradiance levels on growth. Growth rates in response to the experimental treatments
37 varied among isolates, but were generally highest under conditions that included both
38 the shortest photoperiod interval (16h:8h light:dark) and higher irradiance levels
39 ($\sim 146\text{-}366 \mu\text{mol photons m}^{-2} \text{ s}^{-1}$), followed by growth under an extended photoperiod
40 interval and low irradiance level ($\sim 37 \mu\text{mol photons m}^{-2} \text{ s}^{-1}$). Based on field and
41 laboratory data, we hypothesize that blooms in Greenland are primarily derived from
42 advected *Alexandrium* populations, as low bottom temperatures and limited light
43 availability would likely preclude in situ bloom development. In contrast, the bays
44 and fjords in Iceland may provide more favorable habitat for germling cell survival
45 and growth, and therefore may support indigenous, self-seeding blooms.

46

47

48

49 **Introduction**

50 The bloom-forming dinoflagellate genus *Alexandrium* Halim emend Balech
51 (1995) has been extensively studied due to its toxigenicity, particularly those taxa
52 comprising the “*tamarense* species complex”, which includes *A. acatenella*, *A.*
53 *catenella*, *A. excavatum*, *A. fundyense*, *A. tamarense*, and several closely related
54 species formerly assigned to *Protogonyaulax* Taylor. The human illness caused by the
55 toxins produced by *Alexandrium* is known as Paralytic Shellfish Poisoning (PSP),
56 which is widespread in temperate waters around the world.

57 One strategy for the success of this dinoflagellate across such a range of
58 habitats is that the life cycle of many species in this genus includes a benthic cyst
59 stage. This life cycle stage allows cells to enter dormancy during unfavorable
60 temperature or nutrient conditions, and survive in sediments during temperature
61 extremes (i.e., overwinter), with seasonal germination inoculating vegetative cells into
62 the water column only during intervals when conditions are suitable for growth
63 (Anderson, 1998). Population development is thus possible in more locations than
64 would otherwise be the case if year-round persistence in the plankton were the only
65 means for survival. The cyst is also critical in species dispersal, as cells transported to
66 new locations by storms, currents, wildlife, or humans can colonize an area by
67 depositing cysts that germinate in subsequent years.

68 Due to the widespread and serious impacts of these blooms, the distribution,
69 life cycle, taxonomy, and physiology of *Alexandrium tamarense* species complex taxa
70 are relatively well-studied compared with many other globally distributed
71 phytoplankton. Recent morphological, molecular, and mating studies indicate that the
72 strains comprising the Group 1 (formerly North American) clade (Lilly et al. 2007) of
73 this complex comprise a single species – *Alexandrium fundyense* (John et al. 2014a).

74 There is general agreement that the *tamarensis* complex should be split into separate
75 species, but there is some disagreement on the name to be used for that clade, with
76 some arguing that it should be *A. catenella* and not *A. fundyense* (Fraga et al. 2015).
77 Here we use the name *A. fundyense*, but recognize that this issue is not yet fully
78 resolved.

79 Although *A. fundyense* is not considered to be endemic to the Arctic, several
80 recent reports of *Alexandrium* cysts, cells, and toxins from Arctic waters suggest that
81 suitable habitat for growth and bloom formation is present in this region. *Alexandrium*
82 *fundyense* has been reported from coastal waters near Barrow, AK (Okolodkov 2005),
83 and recent work by several groups documented *A. fundyense* cysts, vegetative cells,
84 and toxins in the Chukchi and Beaufort Seas (Gu et al. 2013, Natsuike et al. 2013).
85 Notably, the extraordinarily high densities of *A. fundyense* cysts (maximum 10,600
86 cysts cm⁻³) observed in surface sediments from the Chukchi Sea are among the
87 highest ever reported for this species (Natsuike et al. 2013).

88 In waters east of North America and north of Europe, *A. fundyense* has been
89 observed in plankton samples from the Labrador, Greenland, and Norwegian Seas
90 (Scholin 1998, Okolodkov 2005, Baggesen et al. 2012, Tillmann et al. 2016), and in
91 the Northwest Passage in the Canadian archipelago (M. Levasseur pers. comm.). PSP
92 toxins in blue mussels were recently reported for the first time from Iceland, along
93 with record high numbers of toxic *Alexandrium* spp. (>16,000 cells L⁻¹) (Burrell et al.
94 2013). Additionally, PSP toxins were detected in scallops at levels exceeding
95 regulatory limits for the first time in western Greenland (Baggesen et al. 2012), and *A.*
96 *fundyense* was isolated and identified from nearby waters. Although it is clear that
97 environmental conditions in at least some areas of the Arctic foster cell growth and
98 bloom development, it is yet unclear whether and where the establishment of endemic

99 populations (via cyst germination) might be possible, and how climate-driven
100 increases in bottom temperatures might influence the future range and magnitude of
101 blooms in the region.

102 The aforementioned reports prompted the current investigation, which sought
103 to better characterize the present distribution of this species in western Greenland and
104 Iceland relative to environmental conditions, and to examine growth responses of
105 Arctic isolates compared with those from temperate regions. We examined sediment
106 samples collected in western Greenland and Iceland for *Alexandrium* cyst
107 accumulations, an approach for assessing the presence and magnitude of bloom
108 populations present in previous years, to better understand the prevalence of
109 *Alexandrium* in Arctic waters. Additionally, we characterized the particle size
110 distribution of sediment samples (sediment structure) to assess whether certain areas
111 might favor the accumulation of higher cyst densities.

112 Data collected on the underwater light field, temperature, and sampling depth
113 were used to infer the potential for germling survival and cell growth. Associated
114 laboratory experiments were carried out with *A. fundyense* cultured isolates
115 established during these surveys to examine their growth responses to the particular
116 light intensities and photoperiod intervals that bloom populations would experience
117 during summer months in the Arctic. Our goals were to: (1) provide a preliminary
118 characterization of cyst densities in western Greenland and Iceland, including
119 comparisons between fjord and external coastal habitats, (2) assess environmental
120 factors (temperature, light, and photoperiod interval) that determine viability and
121 growth of germling cells, (3) identify areas that might favor in situ bloom initiation,
122 and (4) use these data to generate hypotheses regarding the origins and fate of PSP-
123 toxin producing *Alexandrium* populations in this region. Many dinoflagellate species

124 form cysts, and thus studies like the one presented here provide information about
125 how this adaptive strategy might influence the distributions of many species in a
126 warming climate.

127

128 **Materials and Methods**

129 *Field collections*

130 Sediment sampling and data collection were carried out during a research
131 oceanographic cruise aboard the *RV Maria S. Merian* (July 27-Aug 8, 2012); see also
132 Cembella et al. (2016). This particular cruise leg (field campaign MSM 21/leg 3)
133 included a comparative study of the west coasts and fjords of Greenland and Iceland
134 (Fig. 1). Sediments were collected from a total of 20 stations to characterize the
135 prevalence of *A. fundyense* cysts in western Greenland and Iceland. Samples in
136 Greenland were collected from Uummannaq Fjord, the Vaigat, and Disko Bay, and
137 from two stations near Cape Farewell, and from Arnarfjörður and Breiðafjörður in
138 Iceland (Fig. 1). Sediments were collected with two Van Veen grab-samplers, each of
139 which can extract sediments up to 20 cm deep, with a sampling area of 0.04 m² (small
140 sampler) or 0.1 m² (large sampler). Samples for cyst enumeration, culture
141 establishment and analysis of sediment characteristics were collected from the
142 sediment surface layer (upper 10 cm) in the grab, and stored in anoxic conditions in
143 the dark and at 2 °C until further processing (Anderson et al. 1987). Subsequent
144 laboratory analyses were carried out at the Woods Hole Oceanographic Institution,
145 Woods Hole, MA, USA.

146 For cyst enumeration, a homogenized 5 cm³ sediment sample was removed
147 from each sample, resuspended with filtered seawater, sonicated with a Branson

148 Sonifier 250D at a constant 40-watt output for one minute, and sieved to yield a clean,
149 20-100 μm size fraction (Anderson et al. 2003). Cysts were then concentrated using a
150 single density layer (1.4 g cm^{-3}) of NALCO 1060 colloidal silica (Nalco Company,
151 IL, USA) (Schwinghamer et al. 1991, Anderson et al. 2003) following procedures
152 described in Vahtera et al. (2014). *Alexandrium fundyense* cysts were stained with
153 primulin (MP Biomedicals, LLC, OH, USA) and enumerated in each sample as
154 described in Anderson et al. (2003).

155

156 *Analysis of sediment structure*

157 Sediment samples were collected at defined stations and frozen at $-25 \text{ }^{\circ}\text{C}$ until
158 analysis at the University of Oldenburg, Oldenburg, Germany. For these analyses, the
159 particle size distribution (PSD) from subsamples was determined using a laser
160 scattering particle size analyzer (Horiba LA-950, Japan). To remove coarse fragments
161 before measurement, subsamples were sieved through a 2 mm mesh sieve and treated
162 with sodium meta-phosphate (NaPO_3 , 2% in water) due to presence of aggregates in
163 the sample. The filtrate was examined with the laser particle size analyzer, which has
164 a measurement range of $0.01 - 3000 \mu\text{m}$, providing relative composition of seven
165 granulometric fractions from $<2 \mu\text{m}$ to $630 - 2000 \mu\text{m}$.

166

167 *Water column properties and optical measurements*

168 At each sampling location data on water column properties were collected
169 with a CTD-rosette sampler, and above-water and in-water hyperspectral radiometric
170 measurements were collected to investigate the optical properties of water masses (see
171 also Garaba & Zielinski 2013, Holinde & Zielinski 2015). The CTD casts were

172 performed with a Seabird “sbe911+” CTD probe with sampling rosette at each station
173 as a start-up to determine further key discrete sampling depths, e.g., to locate
174 chlorophyll maxima. Live data acquisition was carried out via CTD-client onboard
175 and data post-processing with Seasoftware V2 (Seabird, WA, USA). Salinity and depth
176 were calculated from pressure values (UNESCO 1983), and temperature was
177 corrected to ITS-90 (Preston-Thomas 1990). All CTD data are available from the
178 WDC-Mare database system Pangaea@ [doi:10.1594/PANGAEA.819731](https://doi.org/10.1594/PANGAEA.819731).

179 A HyperPro II profiling system (Satlantic, Halifax, Canada) was used to
180 acquire bio-optical data for inherent and apparent optical properties (Holinde &
181 Zielinski 2015). The profiler consisted of one hyperspectral irradiance and one
182 hyperspectral radiance sensor. A second hyperspectral irradiance sensor was mounted
183 at an unshaded elevated position on the research vessel for reference measurements
184 (E_s). On the profiler, the irradiance and radiance sensors measured downwelling (E_d)
185 and upwelling (L_u) light, respectively.

186 Profiler measurements were conducted at selected stations depending on sea,
187 weather, and daylight conditions. At these stations, three casts were typically
188 performed. For each cast, the profiler was lowered until the downwelling light values
189 were of the same order of magnitude as the background noise level of the sensor.
190 Hyperspectral $E_d(\lambda)$ data were then processed with ProSoft 7.7.16 (Satlantic) and
191 binned to 0.2 m depth intervals to calculate photosynthetically active radiation (PAR)

192

193
$$\text{PAR}(z) = \int_{400}^{700} (\lambda/hc) E_d(\lambda) d\lambda$$

194 where z is the depth in meters, λ is the wavelength in nanometers, h is Planck's
195 constant and c is the speed of light. Additionally, the percentage of PAR reaching
196 depth z with reference to $PAR(0^+)$ calculated from $E_s(\lambda)$ was determined according to:

$$197 \quad \%P(z) = PAR(z)/PAR(0^+) \times 100$$

198 Based on $\%PAR(z)$, the 1% depth of PAR, a common indicator for the depth of the
199 euphotic zone, was derived together with the maximum wavelength present at that
200 depth. The mean values of the available profiles were used for all calculated profiler
201 data.

202 *Irradiance and photoperiod experiments*

203 A subset of plankton and sediment samples was also used to establish
204 *Alexandrium* spp. cultures (Supplementary Table S1), either from single cell
205 isolations from plankton samples (Tillmann et al. 2016), or from germinated cysts.
206 Additionally, isolates were established from cysts in sediments collected from the
207 Chukchi Sea, which were kindly provided by Dr. Haifeng Gu (Third Institute of
208 Oceanography, Xiamen, P.R. China). Sediment samples were processed as described
209 above, and cysts were isolated via micropipetting and placed in individual wells of
210 24-well tissue culture plates containing $f/2(-Si)$ growth medium (Guillard & Ryther
211 1962). Plates were incubated for approximately one week at 10 °C under a 14h:10h
212 light:dark photoperiod cycle. Wells were examined daily for germination and once
213 sufficient motile cells were observed, individual cells were isolated, washed, and
214 placed singly into tubes containing $f/2(-Si)$ medium. Cultures were initially
215 maintained at 10 °C, but were subsequently maintained at 15 °C due to improved
216 growth at the higher temperature. Species designations of isolates were determined by

217 sequencing the highly variable D1-D2 domains of the large subunit ribosomal RNA
218 gene (LSU rRNA) (Tillmann et al. 2016; D.M. Anderson unpub. data).

219 A series of laboratory experiments were performed to assess the effects of
220 irradiance and photoperiod interval on growth responses of *A. fundyense* under the
221 particular light conditions that bloom populations would experience during summer in
222 the Arctic. These experiments were carried out with three isolates each from
223 Greenland, Iceland, and the Chukchi Sea; three isolates originating from a temperate
224 location, the Gulf of Maine (GOM), were also examined (Supplementary Table S1).
225 The Greenland isolate E516 died before the experiments could be completed; it was
226 therefore necessary to use a different isolate (P3H8) in the 24h:0h light:dark (L:D)
227 photoperiod treatment (see below). Experiments were performed in an incubator at a
228 constant 12 °C; each isolate was grown in triplicate under irradiance levels of 37, 92,
229 146, 183, 275, and 366 $\mu\text{mol photons m}^{-2} \text{ s}^{-1}$, which were established on four shelves
230 by combining different light settings on each shelf with nylon window screen (1-2
231 layers) to provide additional shading. The lowest irradiance level was selected based
232 on prior studies of *A. fundyense* from the Northwest Atlantic (Etheridge & Roesler
233 2005), in which growth rates in response to irradiance were lowest under 25 and 50
234 $\mu\text{mol photons m}^{-2} \text{ s}^{-1}$ (but at 20 °C, higher than the temperature level used in these
235 experiments).

236 Irradiance received by the cultures was measured with a digital scalar
237 irradiance meter (Model QSP-170, Biospherical Instruments, CA, USA) equipped
238 with a probe QSL-100. Experiments were replicated under three different photoperiod
239 intervals: 24h:0h, 20h:4h, and 16h:8h L:D. Preliminary studies confirmed a linear
240 correlation between in vivo fluorescence and cell concentrations, and population
241 growth was subsequently monitored by in vivo fluorescence measured with a 10-AU

242 fluorometer (Turner Designs, USA) in a 25 mm cuvette. Fluorescence was measured
243 in each tube at the same time (~10:30) three times per week, and tubes were shaken
244 by hand to distribute the cells uniformly in the medium before measuring
245 fluorescence. Growth data were collected from three technical replicates of each
246 isolate.

247 The intrinsic growth rate was calculated over the exponential phase of growth
248 (as inferred from a semi-log plot of fluorescence versus time; see Guillard 1973,
249 Wood et al. 2005) by the following equation:

$$250 \quad \mu = \frac{\ln(N_1/N_0)}{t_1 - t_0}$$

251 in which μ (day^{-1}) represents the growth rate, and N_1 and N_0 represent the
252 fluorescence at times t_1 and t_0 , respectively.

253

254 *Statistical analyses*

255 Statistical analyses to examine the effects of irradiance and photoperiod
256 interval on growth were performed with JMP 11 software (SAS Institute, NC, USA).
257 Datasets were first grouped by region (Greenland, Iceland, Chukchi, GOM) for these
258 analyses. Effects of irradiance on growth were compared among regions, but within
259 each photoperiod interval, and growth response data for each photoperiod interval (at
260 all irradiance levels) were also pooled and compared. Growth data were not normally
261 distributed, and it was not possible to achieve normality by transforming the data;
262 non-parametric Welch's ANOVA and Wilcoxon rank sum tests were used instead for
263 these comparisons, with $\alpha = 0.5$.

264 Additionally, principal components analysis (PCA) was performed with
265 Primer v6.0 (Primer-E, Plymouth, UK) to examine correlations between cyst
266 abundance, components of the sediment structure, and depth, and to evaluate regional
267 clustering among samples.

268

269 **Results**

270 *Temperature profiles and bio-optical parameters*

271 Clear differences in temperature profiles were observed among the sampling
272 locations (Fig. 2). Temperature measured in profiles from Uummannaq Fjord
273 (transect distance 0–200 km), the Vaigat (250–450 km), and Disko Bay (>450 km)
274 generally ranged from ~0–7 °C, and values throughout much of the water column
275 were <4 °C. Maximum temperatures of ~11–12 °C were only found in surface waters
276 at two locations. Cold melt water from the Perlerfiup Sermia glacier at the head of the
277 Perlerfiup Kangerlua, a tributary fjord of the Uummannaq Fjord system, and
278 representing the starting point of the transect, was detected throughout section
279 distance (0–150 km) between 20 and 200 m depth with temperatures <1 °C.

280 Water temperatures in Icelandic fjords were much higher, ranging from 2–12
281 °C in Arnarfjörður and 6–15 °C in Breiðafjörður (Fig. 2). With the exception of the
282 deepest areas of Arnarfjörður (>60 m), water temperatures in this fjord system were
283 generally >8 °C throughout much of the water column.

284 Analysis of light availability from radiometric profiles showed that the 1%
285 PAR depth was <46 m at all stations surveyed, ranging from 15.9 m (St 535) to 45.7
286 m (St 522) (Fig. 1, Table 1). Maximum wavelength at the 1% level was shifted from
287 below 500 nm for all Greenland stations to 530 ± 30 nm for Iceland stations due to

288 increased presence of colored dissolved organic matter (CDOM) absorbing ultraviolet
289 and blue spectral components (data not shown).

290

291 *Distribution and abundance of Alexandrium cysts*

292 *Alexandrium fundyense* resting cysts were observed in sediments from all
293 stations surveyed in Greenland and Iceland, with the exception of St 523 and 524,
294 located near Cape Farewell, Greenland (Fig. 1). Cysts of several other dinoflagellate
295 taxa (*A. minutum*, *A. ostenfeldii*, *Protoceratium* sp., *Protoperidinium* sp., *Scrippsiella*
296 sp.) were also observed (but not quantified) in many of the samples, including those
297 collected from Cape Farewell. Cyst concentrations in sediments collected from the
298 other Greenland stations ranged from 2 to 37 cysts cm⁻³ (mean ± SD: 9 ± 11 cysts cm⁻³)
299 ³), with highest concentrations found in Uummannaq Fjord (Fig. 3). Cyst
300 concentrations in Iceland were higher, ranging from 15 to 408 cysts cm⁻³ (mean ± SD:
301 109 ± 127 cysts cm⁻³). In Iceland, highest cyst concentrations were observed at St 538
302 (408 cysts cm⁻³) in Breiðafjörður, followed by St 529 (124 cysts cm⁻³) and St 537 (120
303 cysts cm⁻³) in Arnarfjörður and Breiðafjörður, respectively (Fig. 3). The sediment
304 sampling regimes differed substantially between Greenland and Iceland stations with
305 respect to sampling depth. In Greenland, samples were collected from depths ranging
306 from 135 to 550 m, with the majority of samples collected at depths >200 m (Fig. 4).
307 In Iceland, however, sampling depths ranged from 51 to 330 m, and all but one
308 sample were collected from depths <200 m.

309 *Sediment characterization*

310 Seven granulometric fractions ranging from <2 to 2000 µm were quantified in
311 each of the sediment samples. The most apparent differences among samples were the

312 higher proportions of fine silt in samples from Greenland compared with those from
313 Iceland (Fig. 5), and the higher proportions of coarser, sandy sediments (F_{63-200} ,
314 $F_{200-630}$) in samples from St 523 and 524, collected near Cape Farewell. With the
315 exception of these two stations, finer sedimentary fractions ($F_{<63}$) comprised 50% or
316 more of the particle size fractions of each sample (Fig. 5).

317 In the principal component analysis (PCA) based upon data on sediment
318 characteristics, water depth, and cyst abundance, the first two principal components
319 accounted for 72.8% of the variance, with the third accounting for an additional
320 11.8%. The strongest correlations (positive or negative) for the first principal
321 component were with $F_{2-6.3}$ and F_{63-200} . For the second principal component, the
322 strongest correlations were with F_{63-200} and cysts cm^{-3} . In the PCA plot, clustering
323 according to region was observed (Fig. 6). The first cluster comprised the samples
324 collected from Iceland and St 516 (Disko Bay, Greenland), whereas the second
325 comprised those from the Cape Farewell stations (St 523 and St 524), and the third
326 comprised the remaining Greenland samples.

327

328 *Photoperiod interval and irradiance experiments*

329 Patterns of growth responses to the experimental treatments varied widely
330 among isolates but were strain- rather than region-specific. In all cases, both
331 photoperiod and irradiance had significant effects on growth, with the highest growth
332 rate (0.28 day^{-1}) observed in these experiments for Iceland isolate D3 grown under
333 constant light (24h:0h L:D) but at the lowest irradiance level (Supplementary Fig. S1).
334 The next highest growth rates were observed for the same isolate grown under
335 constant light, at the next two lowest irradiance levels (~ 92 and $\sim 147 \mu\text{mol photons}$

336 $\text{m}^{-2} \text{s}^{-1}$, respectively. The lowest growth rate (0.016 day^{-1}) determined in this study
337 was observed for both P2H7 (Greenland) and F5 (Chukchi Sea) grown under constant
338 light (24h:0h L:D) and at the highest irradiance level ($\sim 366 \mu\text{mol photons m}^{-2} \text{ s}^{-1}$).
339 The next lowest growth rate was exhibited by isolate E516 (Greenland) under the
340 aforementioned experimental conditions.

341 Although irradiance level had significant effects on growth, these effects
342 varied according to photoperiod interval and among regions. Under the shortest light-
343 period interval (16h:8h L:D), growth rates were generally lowest at the lowest
344 irradiance level, and were significantly higher at moderate and higher irradiance
345 levels (Fig. 7). However, under extended light-period treatments an inverse pattern
346 was observed, whereby growth rates were highest under low and moderate light
347 levels; apparent photoinhibition was most pronounced under constant light treatment
348 (24h:0h L:D) (Fig. 7, Supplementary Fig. S1). Comparison of the combined growth
349 response dataset among regions (data pooled from each irradiance level) showed that
350 regardless of irradiance level, growth rates of isolates from the Chukchi Sea and
351 GOM were significantly higher under the shortest irradiance interval (16h:8h L:D)
352 than under an extended interval (20h:4h L:D) or constant light regime (24h:0h L:D)
353 ($p < 0.05$; Welch's ANOVA; Wilcoxon multiple comparisons). Growth rates of
354 isolates from Greenland grown under the constant light were significantly lower than
355 those grown under the other photoperiod intervals ($p < 0.05$; Welch's ANOVA;
356 Wilcoxon multiple comparisons). In contrast, no statistically significant differences
357 in growth rates were observed among the different photoperiod intervals for the
358 Iceland isolates.

359

360 **Discussion**

361 This is the first effort, to our knowledge, to investigate and compare the
362 abundance and distribution of *Alexandrium fundyense* cysts in bottom sediments of
363 coastal Greenland and Iceland, areas which have been recently impacted by toxic
364 *Alexandrium* blooms. Our surveys of western Greenland and Iceland documented low
365 to moderate *A. fundyense* cyst abundances (~20 to 400 cysts cm⁻³) throughout these
366 regions; notably, cysts were observed at nearly all of stations surveyed, but sediments
367 from Iceland contained substantially more cysts compared with samples from
368 Greenland.

369 Based on the analysis of field data collected during the cruise and results of
370 physiology experiments examining growth responses of Arctic *Alexandrium* isolates,
371 we hypothesize that light availability and temperature regimes in the water column in
372 fjords and coastal areas of Greenland are largely unfavorable for germling survival
373 during transit from bottom waters to the surface, even during summer. However,
374 many areas in Iceland could support germling survival and vegetative cell growth,
375 which indicates that cyst deposits in Iceland may indeed be functioning for in situ
376 bloom initiation. We note that the survival and excystment challenges faced by
377 *Alexandrium* cysts in the deep fjords and cold waters of the Arctic are common to
378 many other cyst-forming dinoflagellate species, and to spore-forming diatoms as well,
379 so there is broad ecological relevance to our findings.

380

381 *Cyst distribution*

382 The accumulation rate and total abundance of cysts at a particular location
383 reflects the net balance between deposition versus advective and germination losses,
384 and is thus affected by bathymetric and hydrographic characteristics and processes

385 that determine bloom and/or cyst retention, as well as external and biological controls
386 of cyst germination and bloom initiation. *Alexandrium* spp. cyst densities ranging
387 from hundreds to thousands of cysts per cubic centimeter of surface sediments have
388 been reported from areas around the world impacted by annual *Alexandrium* blooms
389 and PSP, including the Gulf of Maine (GOM) of Canada and the USA, Puget Sound
390 (USA) in the northeast Pacific, several coastal regions of Japan, and the western
391 Mediterranean (Thau Lagoon, France). In the northwestern Atlantic, densities as high
392 as 2000 cysts cm⁻³ and 6700 cysts cm⁻³ were reported from the Bay of Fundy and
393 GOM, respectively (Anderson et al. 2014), and abundances >12,000 cysts cm⁻³ were
394 observed in the Puget Sound region, in an area known to be a hot spot for PSP toxins
395 in shellfish (Horner et al. 2011). Notably, extraordinarily high *A. fundyense* cyst
396 densities (>10,000 cysts cm⁻³) in the Chukchi Sea were recently reported by Natsuike
397 et al. (2013). However, in contrast with the aforementioned regions in which high cyst
398 densities were generally associated with massive seasonal blooms, cyst concentrations
399 in the Chukchi Sea sediments may well reflect the deposition of cysts year after year
400 during a series of smaller blooms over time (rather than cyst deposition following a
401 major bloom), with little or no germination losses, leading to the high abundances
402 observed. As an example of the magnitude of cyst deposition following a major
403 bloom, McGillicuddy et al. (2014) documented a red-water *A. fundyense* bloom in the
404 GOM (cell densities in excess of 3×10^6 cells L⁻¹) that deposited only 10% as many
405 cysts as observed in Chukchi Sea sediments (Natsuike et al. 2013).

406 With the exception of the two stations near Cape Farewell, *A. fundyense* cysts
407 were found in all Greenland samples collected during the cruise. Cyst accumulations
408 in Greenland sediments were generally low, and the maximum abundance of 37 cysts
409 cm⁻³ was observed in Uummannaq Fjord (Fig. 3). In contrast, much higher cyst

410 abundances were observed in sediments from Iceland, ranging from 15–408 cysts cm⁻³
411 ³. Although cyst accumulations in Greenland and Iceland were low to moderate
412 compared with areas impacted by large-scale, annual *Alexandrium* blooms (e.g.,
413 Anderson et al. 2014), the concentrations we found are well within the range reported
414 from areas with seasonal *Alexandrium* blooms and recurrent PSP toxin accumulation
415 in shellfish. One example of relatively low cyst abundance levels leading to
416 *Alexandrium* blooms comes from the Nauset estuary in Massachusetts, USA, where
417 cyst densities of 150–418 cysts cm⁻³ have been associated with blooms and recurrent
418 PSP-related shellfish harvesting closures in several of the embayments within that
419 system (Crespo et al. 2011). Likewise, in a lagoon-wide survey of the Thau Lagoon in
420 France, which is impacted annually by PSP toxin contamination in shellfish, the mean
421 density of *Alexandrium* cysts was relatively low (<20 cysts g⁻¹ dry sediment [DS]),
422 with the highest density (~440 cysts g⁻¹ DS) recorded at one location within the
423 system where dense blooms were previously observed (Genovesi et al. 2013). Using
424 the relationship between cyst abundance normalized to sediment dry weight versus
425 sediment volume determined for *A. fundyense* in the GOM (Anderson et al. 2014),
426 these Thau Lagoon values equate to 34–185 cysts cm⁻³. The GOM relationship may
427 not be entirely appropriate for Thau Lagoon because of differences in sediment
428 consistency and granularity, but is considered suitable for a rough approximation of
429 cyst cm⁻³ levels.

430

431 *Sediment structure*

432 Although cyst distributions are frequently heterogeneous and sites-specific, prior
433 investigations seeking to better define the physical dynamics underlying the
434 occurrence of cyst seedbeds have identified several important characteristics common

435 to many important cyst accumulation zones. First and perhaps most importantly,
436 higher cyst densities have been reported from protected or enclosed areas such as
437 fjords, embayments, and harbors (Anderson 1997, Godhe & McQuoid 2003, Crespo
438 et al. 2011), which serve to entrain blooms and promote local cyst deposition. Cyst
439 abundance is also positively correlated with the proportion of finer grains and levels
440 of total organic carbon (TOC) in sediments (Horner et al. 2011, Genovesi et al. 2013,
441 Anderson et al. 2014). Finally, higher abundances have been linked with higher
442 summer surface water temperature, which serves to stimulate dinoflagellate growth
443 and promote the vertical stratification of the water column (Godhe & McQuoid 2003),
444 leading to both a higher potential inoculum and reduced advective loss of cells within
445 the system.

446 Dale (1976) first proposed that cysts tend to behave as fine silt particles in
447 sediment dynamics, and as such, increase in abundance as the proportional abundance
448 of finer sediment increases (often at depth). This hypothesis is supported by reports
449 of higher *Alexandrium* spp. cyst accumulations in finer sediments or mud compared
450 with sandy areas (Nehring 1994, Gayoso 2001, Yamaguchi et al. 2002, Anderson et
451 al. 2005), and by subsequent investigations of the correlation between cyst densities
452 and sediment characteristics. In surveys of Puget Sound, Washington, USA, Horner et
453 al. (2011) observed a positive correlation between cyst abundance and the percentage
454 of clay and silt in sediments during small scale surveys in Quartermaster Harbor,
455 located in the south basin of Puget Sound. This pattern was not observed, however, in
456 the large scale, sound-wide surveys, potentially due to variable and site-specific
457 physical forcing conditions within the system (Moore et al. 2008, Horner et al. 2011).

458 Genovesi et al. (2013) documented a significant correlation between
459 *Alexandrium* cyst densities and the *F20–50* sediment fraction in the Thau Lagoon,

460 along the French Mediterranean coast, and reported that the cysts in this ecosystem
461 effectively behaved like 20 to 50 μm particles (the approximate size range of
462 *Alexandrium* cysts). With the exception of the two stations sampled near Cape
463 Farewell, sediments in Greenland and Iceland were characterized by a high proportion
464 of finer grained sediment fractions ($<63 \mu\text{m}$) (Fig. 5), and would thus favor cyst
465 accumulations in these areas. The most apparent difference among locations was the
466 higher proportion of fine silt ($<2 \mu\text{m}$) in the majority of samples collected from
467 Greenland (Uummannaq and Disko Bay) compared with those from Iceland. These
468 very fine particles, also referred to as glacial flour, are transported to the estuary with
469 the melt water (Lund-Hansen et al. 2010). A second apparent difference was the
470 higher proportion of coarser, sandy sediments ($>63 \mu\text{m}$) in samples from St 523 and
471 524. Both stations are located near Cape Farewell on the southern coast of Greenland,
472 and are typically exposed to open sea conditions with higher turbulent energy, thus
473 preventing the accumulation of finer sediments. Notably, these were the only samples
474 in which *Alexandrium* cysts were absent. Regional differences were also evident in
475 the PCA of data on the sediment structure, cyst densities, and sampling depth (Fig. 6).
476 This analysis identified at least three major clusters, grouped according to
477 geographical region. One exception was St. 516 (Disko Bay), which clustered with
478 stations sampled from Iceland in the PCA plot (Fig. 6), and was characterized by a
479 lower proportion of sediment fractions $<6.3 \mu\text{m}$ and a higher proportion of fractions $>$
480 $63 \mu\text{m}$ compared with the other samples from Uummannaq, Disko Bay, and the
481 Vaigat (Fig. 5). This analysis also linked depth with the finest sediment fractions
482 ($<6.3 \mu\text{m}$), whereas cyst densities were linked with the intermediate ($F_{6.3-63}$) and
483 coarsest size fraction ($F_{630-2000}$), the latter of which was only found in samples
484 collected from St 516 and St 530 (Arnarfjörður).

485

486 *Water temperature, depth, and bio-optical parameters*

487 Cyst germination, and subsequent germling cell survival and growth, are
488 highly dependent on light availability and temperature (Anderson 1980, Rengefors &
489 Anderson 1998, Kremp & Anderson 2000, Vahtera et al. 2014); thus, the striking
490 differences in these water column characteristics observed among sampling sites
491 suggest that bloom development might only occur at certain locations within the study
492 area. Temperatures throughout much of the water column in Greenland were
493 generally <4 °C, with the maximum temperature of ~12 °C only detected in surface
494 waters at two locations (Fig. 2). Previous temperature measurements from Disko Bay
495 during the summer months (June-August) ranged from ~4-7 °C (Madsen et al. 2001,
496 Heide-Jørgensen et al. 2007), thus the frequency and extent of the warmer surface
497 waters we documented (>10 °C) is yet unknown. In contrast, water column
498 temperatures measured in Iceland were much higher, ranging from 2 to 12 °C in
499 Arnarfjörður and 6 to 15 °C in Breiðafjörður; with the exception of the deepest areas
500 of Arnarfjörður (>60 m), water temperatures were generally >8 °C. Notably, Burrell
501 et al. (2013) observed high cell concentrations (>10,000 cells L⁻¹) of *Alexandrium*
502 spp., which they tentatively designated as *A. tamarense* along with small numbers of
503 *A. ostenfeldii*, in Breiðafjörður and in Eyjafjordur (northern Iceland) in 2009. Low to
504 moderate *Alexandrium* spp. cell concentrations were also observed in Breiðafjörður
505 and Eyjafjordur from 2005-2008 (Gudfinnsson et al. 2010, Burrell et al. 2013),
506 indicating that blooms may be recurrent at these locations.

507 Differences in bio-optical properties affecting light availability and quality
508 over depth are important determinants of photosynthetically driven growth potential
509 among *Alexandrium* populations at various locations. Based on the results of our

510 laboratory experiments, variation in day length expected in the study region would be
511 most likely to promote growth in August, during which highest seawater temperatures
512 would also be expected. Day length during summer months (July-August) in western
513 Greenland (Disko Bay) and Iceland ranges from >20 hours during much of July, to
514 between ~15-20 hours in August. In our laboratory experiments, highest growth rates
515 were measured at irradiance levels of $\sim 150 \mu\text{mol photons m}^{-2} \text{ s}^{-1}$ or greater under the
516 16 h photoperiod interval. However, the comparatively high growth rates were also
517 observed at low light levels under extended light-period treatments, indicating that
518 longer photoperiod intervals may also be suitable for growth.

519 The 1% depth of PAR derived from our field data was interpreted to indicate
520 the lowest depth of sufficient light for positive *Alexandrium* cell growth in the study
521 region. In general, 1% PAR was surface bound to the upper water column, and was
522 restricted to the top 50 m and 35 m for Greenland and Iceland, respectively (Table 1).
523 Considering water depth, we inferred that the distance to be covered by vertically
524 motile germling cells from bottom water to reach sufficient light for positive growth
525 ranges from <70 m for most Iceland fjord stations to 500 m for St 515, the deepest
526 Greenland station in this dataset. Assuming an average swimming speed of 10 m day⁻¹
527 (Eppley et al. 1968, Bauerfeind et al. 1986, Kamykowski et al. 1992) cells
528 germinating at depths of 70 m would require approximately seven days to reach the
529 surface, whereas cells germinating at 500 m would require 50 days. These transit
530 times may be shorter, however, during upwelling conditions, which could rapidly
531 transport cells to surface waters. The ability of germling cells to survive vertical
532 transit to the euphotic zone in these areas will determine the potential for bloom
533 initiation at these locations (see below).

534

535 *Cyst viability and germling cell survival*

536 Whether or not *A. fundyense* cysts in the Arctic and sub-Arctic (Greenland,
537 Iceland, Chukchi Sea) are able to germinate, and corresponding vegetative cells to
538 transit to the euphotic zone, under the particular temperature and light conditions
539 present (i.e., very cold, deep, and dark waters) to initiate in situ blooms remains
540 unknown. If not, the observed cyst deposits could represent end points or terminal
541 deposits, with the bloom populations that ultimately produce those cysts originating
542 from subarctic systems in the south through transport by coastal currents.
543 Alternatively, cyst deposits from nearby shallow areas could serve as an initiation site
544 for local blooms that lead to deposits in the deeper fjord sections.

545 To our knowledge, the potential for cyst germination and cell growth of *A.*
546 *fundyense* (or any cyst-forming dinoflagellate) from Arctic and subarctic regions have
547 not been studied. At high latitudes, cyst behavior and germling survival and growth at
548 low temperatures and under an extended light-period interval in summer are of
549 fundamental importance to bloom development and life cycle completion. Low
550 temperatures can maintain cyst quiescence for extended periods (months, years, even
551 decades) after cyst deposition and where germination is possible will also regulate the
552 rate of excystment. Following excystment, the germling cell must survive the transit
553 to surface waters, which is influenced by distance travelled in the dark (depth),
554 availability of temperature and light, and cellular energy reserves (Vahtera et al.
555 2014). For the *A. fundyense* strains tested thus far from temperate waters, cyst
556 germination either did not occur or proceeded at extremely low rates at temperatures
557 between 0 and 4 °C (Anderson & Morel 1979, Anderson 1980). Based on the CTD
558 measurements collected during our surveys, bottom temperatures in Greenland are
559 expected to be in this range or lower during much of the potential *Alexandrium* bloom

560 season (Fig. 2). Anderson et al. (2005) showed that at 2 °C, *A. fundyense* cysts from
561 the GOM required up to two months of incubation to reach 50% germination, whereas
562 at 8 °C, this only took one to two weeks. At the low rates expected for cold Arctic
563 waters, the bloom inoculum from excystment would be very gradual and slow, and
564 might therefore introduce cells into the water too late in the season for successful
565 bloom formation and new cyst deposition.

566 Following excystment, temperature and light are both important limiting
567 factors that determine germling survival and vegetative cell growth. For many *A.*
568 *fundyense* strains, including the few isolates examined from Greenland, Iceland, and
569 the Chukchi Sea, a temperature range for survival and growth of 2 to 24 °C has been
570 observed, with rates that are <25% of maxima at 6 °C or less (Watras et al. 1982;
571 Anderson and Rengefors 2006; D.M. Anderson unpub. data). Although they were
572 collected from Arctic and sub-arctic locations, the isolates we examined did not
573 appear to be physiologically adapted for growth and survival in the extremely cold
574 bottom water temperatures in the Arctic. Instead, their growth responses to
575 temperature were similar to those of temperate isolates, with the maximum growth
576 rate for all isolates found between 16–18 °C. These data will be published separately,
577 along with a detailed analysis of the toxin contents of these isolates (Tillmann et al.
578 2016; D.M. Anderson unpub. data). The CTD temperature profiles collected during
579 the cruise indicated that summer water temperatures in the Uummannaq/Disko Bay
580 region only ranged from 4 to 8 °C, well below the temperature range for optimal
581 growth, and bottom temperatures were much lower (Fig. 2).

582 Furthermore, the depth from which sediments were collected suggests that
583 the survival of germinated cysts would be low at many of the locations surveyed in
584 Greenland. Laboratory experiments examining the effects of dark treatment on cyst

585 germination and survival estimated that <50% of germinated cells would survive a 70
586 m transit from bottom sediments to the surface, and only 20% could survive a 200 m
587 ascent in the dark (Vahtera et al. 2014). In Iceland, the estimated distances germlings
588 would have to travel from germination depth to reach the 1% PAR depth ranged from
589 13 to 167 m; however, these estimated distances are substantially greater in
590 Greenland, where the travel distance from germination depth to 1% PAR ranged from
591 68 to 503 m. Using the equations derived by Vahtera et al. (2014) describing the
592 depth-related mortality rate, and assuming an initial survival time of one day, the
593 proportions of cells estimated to survive the transit from the germination depth to 1%
594 PAR ranged from 14 to 26% in Greenland, and 18 to 82% in Iceland.

595 Based on these field and experimental data, it is likely that *Alexandrium* cells
596 and associated toxins in shellfish from Greenland are primarily derived from advected
597 *Alexandrium* populations. There may also be certain shallow, nearshore areas,
598 however, not explored in this study, that could provide favorable habitat for cyst
599 germination and germling survival. Conditions in the bay and fjords we surveyed in
600 western Iceland are suitable for germling survival and vegetative cell growth, and
601 therefore may support indigenous, self-seeding blooms. The potential for
602 *Alexandrium* bloom initiation in Greenland and other Arctic areas may be enhanced in
603 the future, as Arctic Ocean bottom temperatures are projected to increase at a rate of 1
604 to 5 °C per 100 years, with a higher rate in nearshore regions (Bjastoch et al. 2011).
605 This will clearly have an impact on the germination and survival rate of *Alexandrium*,
606 but also will affect the distribution and bloom timing of many other meroplanktonic
607 phytoplankton species.

608

609 **Conclusions**

610 Our field investigation documented low to moderate densities of *Alexandrium*
611 cysts in most areas surveyed in Greenland and Iceland, with highest densities
612 observed in western Iceland. We know that *A. fundyense* strains disperse readily and
613 are highly adaptable to new regions due to their ability to form cysts, overwinter, and
614 germinate to initiate blooms. Based on data collected on the temperature and light
615 availability (as influenced by water depth), we hypothesize that blooms in Greenland
616 are primarily derived from advected *Alexandrium* populations, as extremely low
617 bottom temperatures and travel distance from germination depth to the euphotic zone
618 would preclude in situ bloom initiation at most of the locations we surveyed.
619 Alternatively, cyst deposits from nearby shallow areas could serve as an initiation of
620 local blooms that lead to deposits in the deeper fjord sections. We further hypothesize
621 that in contrast with the situation in Greenland, the bays and fjords in Iceland provide
622 favorable habitat for germling cell survival and growth, and therefore may support
623 indigenous, self-seeding blooms.

624 The potential for *Alexandrium* blooms in Greenland and other Arctic areas
625 may change, as projected increases in water temperatures could expand habitat
626 suitable for *Alexandrium* germling survival and cell growth, particularly at nearshore
627 locations. The human health and ecosystem impacts of this potential expansion will
628 be significant, as marine bioresources are extremely important to the economies of
629 both Greenland and Iceland. Additional studies are needed to examine the physiology
630 of *Alexandrium* cysts and cells from the Arctic, particularly with regard to the
631 potential for cyst germination under ambient conditions in the region. These data will
632 help to further characterize processes that determine the distribution of endemic
633 versus introduced populations of *Alexandrium* and other toxin-producing

634 phytoplankton in the Arctic, and will be useful for understanding the potential for
635 dispersal in the region under warmer conditions.

636

637 ACKNOWLEDGEMENTS

638 Funding for this study was provided by the James M. and Ruth P. Clark Arctic
639 Research Initiative to Anderson and Richlen, and for the ARCHEMHAB expedition
640 via the Helmholtz Institute initiative Earth and Environment under the PACES
641 Program Topic 2 Coast (Workpackage 3) of the Alfred Wegener Institute. The
642 research is part of the SCOR/IOC GEOHAB Core Research Project on HABs in
643 Fjords and Coastal Embayments, Additional support was provided by the Woods Hole
644 Center for Oceans and Human Health through National Science Foundation (NSF)
645 Grant OCE-1314642 and National Institute of Environmental Health Sciences
646 (NIEHS) Grant 1-P01-ES021923-01. We are grateful to Daniela Voß, Daniela Meier,
647 and Rohan Henkel for their assistance during the cruise, and for helping to prepare the
648 figures. We also thank Prof. Haifeng Gu for providing sediments from the Chukchi
649 Sea, and Kerry Norton, Dave Kulis, John Brinckerhoff, Bruce Keafer, Lauren Henry,
650 Hovey Clifford, and Judy Kleindinst for logistical and laboratory support and
651 assistance. Finally, we acknowledge the generous support and assistance provided by
652 Captain Klaus Bergman and crew of the Maria S. Merian throughout the cruise.

653

654

655

656

657

658

659 **References**

- 660 Anderson DM (1980) Effects of temperature conditioning on development and germination of
661 *Gonyaulax tamarensis* (Dinophyceae) hypnozygotes. *Journal of Phycology* 16:166-172
- 662 Anderson DM (1997) Bloom dynamics of toxic *Alexandrium* species in the northeastern U.S.
663 *Limnology and Oceanography* 42:1009-1022
- 664 Anderson DM, Fukuyo Y, Matsuoka K (2003) Cyst methodologies. In: Hallegraeff GM (ed) Manual on
665 harmful marine microalgae, Book 11. UNESCO, Monographs on Oceanographic
666 Methodology
- 667 Anderson DM, Keafer BA, Kleindinst JL, McGillicuddy Jr DJ, Martin JL, Norton K, Pilskaln CH,
668 Smith JL, Sherwood CR, Butman B (2014) *Alexandrium fundyense* cysts in the Gulf of
669 Maine: Long-term time series of abundance and distribution, and linkages to past and future
670 blooms. *Deep Sea Research Part II: Topical Studies in Oceanography* 103:6-26
- 671 Anderson DM, Morel FMM (1979) The seeding of two red tide blooms by the germination of benthic
672 *Gonyaulax tamarensis* hypnocysts. *Estuarine and Coastal Marine Science* 8:279-293
- 673 Anderson DM, Stock CA, Keafer BA, Bronzino Nelson A, Thompson B, McGillicuddy JDJ, Keller M,
674 Matrai PA, Martin J (2005) *Alexandrium fundyense* cyst dynamics in the Gulf of Maine. *Deep*
675 *Sea Research Part II: Topical Studies in Oceanography* 52:2522-2542
- 676 Anderson DM, Taylor CD, Armbrust EV (1987) The effects of darkness and anaerobiosis on
677 dinoflagellate cyst germination. *Limnology and Oceanography* 32:340-351
- 678 Baggesen C, Moestrup Ø, Daugbjerg N, Krock B, Cembella AD, Madsen S (2012) Molecular
679 phylogeny and toxin profiles of *Alexandrium tamarensis* (Lebour) Balech (Dinophyceae) from
680 the west coast of Greenland. *Harmful Algae* 19:108-116
- 681 Bauerfeind E, Elbrächter M, Steiner R, Thronsen J (1986) Application of Laser Doppler Spectroscopy
682 (LDS) in determining swimming velocities of motile phytoplankton. *Marine Biology* 93:323-
683 327
- 684 Biastoch A, Treude T, Rüpke LH, Riebesell U, Roth C, Burwicz EB, Park W, Latif M, Böning CW,
685 Madec G, Wallmann K (2011) Rising Arctic Ocean temperatures cause gas hydrate
686 destabilization and ocean acidification. *Geophysical Research Letters* 38:L08602
- 687 Burrell S, Gunnarsson T, Gunnarsson K, Clarke D, Turner AD (2013) First detection of paralytic
688 shellfish poisoning (PSP) toxins in Icelandic mussels (*Mytilus edulis*): Links to causative
689 phytoplankton species. *Food Control* 31:295-301
- 690 Cembella A, Zielinski O, Anderson D, Graeve M, Henkel R, John U, Kattner G, Koch B, Krock B,
691 Meier D, Richlen M, Tillmann U, Voß D (2016) ARCHEMHAB: Interactions and feedback
692 mechanisms between hydrography, geo-chemical signatures and microbial ecology, with a
693 focus on HAB species diversity, biogeography and dynamics Cruise Report MSM21/3, DFG-
694 Senatskommission für Ozeanographie, Bremen, Germany, 51 pages
- 695 Crespo BG, Keafer BA, Ralston DK, Lind H, Farber D, Anderson DM (2011) Dynamics of
696 *Alexandrium fundyense* blooms and shellfish toxicity in the Nauset Marsh System of Cape
697 Cod (Massachusetts, USA). *Harmful Algae* 12:26-38
- 698 Dale B (1976) Cyst formation, sedimentation, and preservation: Factors affecting dinoflagellate
699 assemblages in recent sediments from trondheimsfjord, Norway. *Review of Palaeobotany and*
700 *Palynology* 22:39-60
- 701 Eppley RW, Holm-Harisen O, Strickland JDH (1968) Some observations on the vertical migration of
702 dinoflagellates S. *Journal of Phycology* 4:333-340
- 703 Etheridge SM, Roesler CS (2005) Effects of temperature, irradiance, and salinity on photosynthesis,
704 growth rates, total toxicity, and toxin composition for *Alexandrium fundyense* isolates from
705 the Gulf of Maine and Bay of Fundy. *Deep Sea Research Part II: Topical Studies in*
706 *Oceanography* 52:2491-2500
- 707 Fraga S, Sampedro N, Larsen J, Moestrup Ø, Calado AJ (2015) Arguments against the proposal 2302
708 by John & al. to reject the name *Gonyaulax catenella* (*Alexandrium catenella*). *Taxon* 64:634-
709 635
- 710 Garaba SP, Zielinski O (2013) Comparison of remote sensing reflectance from above-water and in-
711 water measurements west of Greenland, Labrador Sea, Denmark Strait, and west of Iceland.
712 *Opt Express* 21:15938-15950, doi: 15910.11364/OE.15921.015938
- 713 Gayoso AM (2001) Observations on *Alexandrium tamarensis* (Lebour) Balech and other dinoflagellate
714 populations in Golfo Nuevo, Patagonia (Argentina). *Journal of Plankton Research* 23:463-468
- 715 Genovesi B, Mouillot D, Laugier T, Fiandrino A, Laabir M, Vaquer A, Grzebyk D (2013) Influences of
716 sedimentation and hydrodynamics on the spatial distribution of *Alexandrium*

- 717 *catenella/tamarensis* resting cysts in a shellfish farming lagoon impacted by toxic blooms.
718 Harmful Algae 25:15-25
- 719 Godhe A, McQuoid MR (2003) Influence of benthic and pelagic environmental factors on the
720 distribution of dinoflagellate cysts in surface sediments along the Swedish west coast. Aquatic
721 Microbial Ecology 32:185-201
- 722 Gu H, Zeng N, Xie Z, Wang D, Wang W, Yang W (2013) Morphology, phylogeny, and toxicity of
723 Atama complex (Dinophyceae) from the Chukchi Sea. Polar Biol 36:427-436
- 724 Gudfinnsson HG, Eydal A, Gunnarsson K, Gudmundsson K, Valsdóttir K (2010) Monitoring of toxic
725 phytoplankton in three Icelandic fjords. ICES theme session N
- 726 Guillard RR, Ryther JH (1962) Studies of marine diatoms. I. *Cyclotella nana* Husdedt and *Detonula*
727 *confervacea* Gran. . Can J Microbiol 8:229-239
- 728 Guillard RRL (1973) Division rates. In: Stein JR (ed) Handbook of phycological methods. Cambridge
729 Univ. Press
- 730 Heide-Jørgensen MP, Laidre KL, Logsdon ML, Nielsen TG (2007) Springtime coupling between
731 chlorophyll a, sea ice and sea surface temperature in Disko Bay, West Greenland. Progress in
732 Oceanography 73:79-95
- 733 Holinde L, Zielinski O (2015) Bio-optical characterization and light availability parameterization in
734 Uummannaq Fjord and Vaigat–Disko Bay (West Greenland). Ocean Science 12:117-128,
735 doi:10.5194/os-5112-5117-2016.
- 736 Horner RA, Greengrove CL, Davies-Vollum KS, Gawel JE, Postel JR, Cox AM (2011) Spatial
737 distribution of benthic cysts of *Alexandrium catenella* in surface sediments of Puget Sound,
738 Washington, USA. Harmful Algae 11:96-105
- 739 John U, Litaker RW, Montresor M, Murray S, Brosnahan ML, Anderson DM (2014a) Formal Revision
740 of the *Alexandrium tamarensis* Species Complex (Dinophyceae) Taxonomy: The Introduction
741 of Five Species with Emphasis on Molecular-based (rDNA) Classification. Protist 165:779-
742 804
- 743 John U, Litaker W, Montresor M, Murray S, Brosnahan ML, Anderson DM (2014b) (2302) Proposal to
744 reject the name *Gonyaulax catenella* (*Alexandrium catenella*)(Dinophyceae). Taxon 63:932
- 745 Kamykowski D, Reed RE, Kirkpatrick GJ (1992) Comparison of sinking velocity, swimming velocity,
746 rotation and path characteristics among six marine dinoflagellate species. Marine Biology
747 113:319-328
- 748 Kremp A, Anderson DM (2000) Factors regulating germination of resting cysts of the spring bloom
749 dinoflagellate *Scrippsiella hangoei* from the northern Baltic Sea. Journal of Plankton Research
750 22:1311-1327
- 751 Lilly EL, Halanych KM, Anderson DM (2007) Species boundaries and global biogeography of the
752 *Alexandrium tamarensis* complex (Dinophyceae). Journal of Phycology 43:1329-1338
- 753 Lund-Hansen LC, Andersen TJ, Nielsen MH, Pejrup M (2010) Suspended matter, Chl-a, CDOM, grain
754 sizes, and optical properties in the Arctic fjord-type estuary, Kangerlussuaq, West Greenland
755 during summer. Estuaries and coasts 33:1442-1451
- 756 Madsen SD, Nielsen TG, Hansen BW (2001) Annual population development and production by
757 *Calanus finmarchicus*, *C. glacialis* and *C. hyperboreus* in Disko Bay, western Greenland.
758 Marine Biology 139:75-93
- 759 McGillicuddy Jr DJ, Brosnahan ML, Couture DA, He R, Keafer BA, Manning JP, Martin JL, Pilskaln
760 CH, Townsend DW, Anderson DM (2014) A red tide of *Alexandrium fundyense* in the Gulf of
761 Maine. Deep Sea Research Part II: Topical Studies in Oceanography 103:174-184
- 762 Moore SK, Mantua NJ, Kellogg JP, Newton JA (2008) Local and large-scale climate forcing of Puget
763 Sound oceanographic properties on seasonal to interdecadal timescales. Limnol Oceanogr
764 53:1746-1758
- 765 Natsuike M, Nagai S, Matsuno K, Saito R, Tsukazaki C, Yamaguchi A, Imai I (2013) Abundance and
766 distribution of toxic *Alexandrium tamarensis* resting cysts in the sediments of the Chukchi Sea
767 and the eastern Bering Sea. Harmful Algae 27:52-59
- 768 Nehring S (1994) Spatial distribution of dinoflagellate resting cysts in recent sediments of Kiel Bight,
769 Germany (Baltic Sea). Ophelia 39:137-158
- 770 Okolodkov YB (2005) The global distributional patterns of toxic, bloom dinoflagellates recorded from
771 the Eurasian Arctic. Harmful Algae 4:351-369
- 772 Preston-Thomas H (1990) The International Temperature Scale of 1990 (ITS-90). Metrologia 27.1:3-10
- 773 Rengefors K, Anderson DM (1998) Environmental and endogenous regulation of cyst germination in
774 two freshwater dinoflagellates. Journal of Phycology 34:568-577
- 775 Scholin CA (1998) Morphological, genetic and biogeographic relationships of *Alexandrium tamarensis*,
776 *A. catenella* and *A. fundyense*. In: Anderson DM, Hallegraeff GM, Cembella AD (eds) The

777 Physiological Ecology of Harmful Algal Blooms. NATO Advanced Study Institute Series,
778 Springer-Verlag, Heidelberg
779 Schwinghamer P, Anderson DM, Kulis DM (1991) Separation and concentration of living
780 dinoflagellate resting cysts from marine sediments via density-gradient centrifugation. *Limnol*
781 & *Oceanogr* 36:588-295
782 Tillmann U, Krock B, Alpermann TJ, Cembella A (2016) Bioactive compounds of marine
783 dinoflagellate isolates from western Greenland and their phylogenetic association within the
784 genus *Alexandrium*. *Harmful Algae* 51:67-80
785 UNESCO (1983) Algorithms for computation of fundamental properties of seawater UNESCO
786 technical papers in marine science, 44
787 Vahtera E, Crespo BG, McGillicuddy DJ, Olli K, Anderson DM (2014) *Alexandrium fundyense* cyst
788 viability and germling survival in light vs. dark at a constant low temperature. *Deep Sea*
789 *Research Part II: Topical Studies in Oceanography* 103:112-119
790 Watras CJ, Chisholm SW, Anderson DM (1982) Regulation of growth in an estuarine clone of
791 *Gonyaulax tamarensis* Lebour: salinity-dependent temperature responses. *Journal of*
792 *Experimental Marine Biology and Ecology* 62:25-37
793 Wood AM, Everroad R, Wingard L (2005) Measuring growth rates in microalgal cultures. In:
794 Anderson RA (ed) *Algal culturing techniques*. Elsevier Academic Press, Burlington, MA
795 Yamaguchi M, Itakura S, Nagasaki K, Kotani Y (2002) Distribution and abundance of resting cysts of
796 the toxic *Alexandrium* spp. (Dinophyceae) in sediments of the western Seto Inland Sea, Japan.
797 *Fisheries Science* 68:1012-1019
798

799

800

801

802

803

804

805

806

807

808

809

810

811

812

813

814 **FIGURE LEGENDS**

815

816 **Figure 1.** Map showing sediment sampling locations in Greenland and Iceland.
817 Intensive sampling was carried out in the Disko Bay region (DB) and western Iceland
818 (WI).

819

820 **Figure 2.** CTD profiles over the section distance in kilometers for temperature (°C)
821 within selected sections in Greenland (Disko Bay region, top panel) and Iceland
822 (Arnarfjörður and Breiðafjörður; middle and bottom panels, respectively). Stations
823 identified by grey vertical lines. Greenland: starting point was the innermost station
824 in Uummanaq fjord (Perlerfiup Sermia glacier). Vaigat was entered at section
825 distance 250 km and Disko Bay at section distance 450 km. Arnarfjörður: starting
826 point was the innermost station of the fjord. Breiðafjörður: starting point was the
827 innermost station of the fjord.

828

829 **Figure 3.** Abundance and distribution of *Alexandrium fundyense* resting cysts (cysts
830 cm^{-3}) in sediments collected from Greenland (DB=Disko Bay region) and Iceland
831 (WI=West Iceland).

832

833 **Figure 4.** *Alexandrium fundyense* cyst abundance (cysts cm^{-3}) in sediments collected
834 from Greenland and Iceland versus sampling depth.

835

836 **Figure 5.** Proportion of each sediment class in samples collected from Greenland and
837 Iceland. A total of seven granulometric fractions (μm) were quantified. Sampling

838 locations: Uq=Uummannaq; Vg=Vaigat; DB=Disko Bay; CF=Cape Farewell; Af=
839 Arnarfjörður; Bf=Breiðafjörður.

840

841 **Figure 6.** Principal component analysis (PCA) of *Alexandrium* cyst abundance,
842 sediment characteristics, and sampling depth of sediments collected from Greenland
843 (Uummannaq, Vaigat, Disko Bay, Cape Farewell) and Iceland (Arnarfjörður,
844 Breiðafjörður). Stations in Greenland and Iceland are delineated by solid and dashed
845 lines, respectively. Symbols denote specific sampling locations.

846

847 **Figure 7.** Growth rates (μ [day^{-1}]) of *Alexandrium fundyense* isolates from Greenland
848 (n=3), Iceland (n=3), the Chukchi Sea (n=3), and the Gulf of Maine (n=3) in response
849 to irradiance. Data from three different photoperiod intervals (L:D) are shown:
850 16h:8h (solid circles), 20h:4h (open triangles), and 24h:0 (shaded squares).

851

852 **Supplementary Figure S1.** Growth rates (μ [day^{-1}]) of *Alexandrium fundyense*
853 isolates from Greenland (n=3), Iceland (n=3), the Chukchi Sea (n=3), and the Gulf of
854 Maine (n=3) in response to irradiance and photoperiod interval. Data from three
855 different photoperiod intervals (L:D) are shown: 16h:8h (top row), 20h:4h (middle
856 row), and 24h:0 (bottom row).

857

858

859

860

1 **TABLES**

2 **Table 1.** Light availability from radiometric profiles. 1% PAR is the 1% depth level (m) of photosynthetically active radiation PAR(z) (μmol
 3 photons $\text{m}^{-2} \text{s}^{-1}$) with respect to surface PAR(0⁺). $\lambda_{\text{max}1\%}$ is the maximum wavelength observed at that depth. Water depth is the bottom depth of
 4 the respective station. All values are the mean of two to three profiler casts at the specific stations. “*” denotes stations where *Alexandrium* cysts
 5 were quantified.

Station	Location	Water depth (m)	1% PAR	PAR(0+)	Lambda_max1%
503*	Uummanaq, Greenland	402.0	38.0	557	496
504*		350.0	35.7	194	496
506*		143.9	32.8	189	496
514*	Disko Bay, Greenland	259.1	41.3	78	492
515*		543.7	40.3	1291	495
516*		169.5	33.2	354	499
517	West Greenland coast	112.6	41.5	166	496
521		114.7	36.3	1076	496
522		113.2	45.7	1201	495
527*	Arnarfjörður, Iceland	54.0	24.6	332	541
528*		106.2	28.5	461	536
529*		103.2	27.8	289	538

530*		81.0	27.1	287	539
531		46.2	33.4	81	498
532	Breiðafjörður, Iceland	47.0	34.4	131	497
533		53.2	29.7	475	502
534		69.2	20.3	760	565
535*		55.6	15.9	366	567
536		34.2	19.6	88	563
537*		126.6	20.3	676	564
538*		189.9	22.5	966	562

1

2

3

4

5

6

7

8

1

2 **Supplementary Table S1.** Details regarding isolates used to characterize growth
3 responses to light intensity and photoperiod interval.

Isolate	Origin	Year	Isolation method
E516	Disko Bay, Greenland	2012	Single cell from cyst germination
P2E6		2012	Single vegetative cell
P2H7		2012	
P3H8		2012	
E9	Arnarfjörður, Iceland	2012	Single cell from cyst germination
D3		2012	
B10	Breiðafjörður, Iceland	2012	Single cell from cyst germination
GOM H15	Gulf of Maine	2005	Single vegetative cell
GOM D2		2005	
GOM F14		2005	
F5	Chukchi	2013	Single cell from cyst germination
C7		2013	
E2		2013	

4

5

6

7

8

9

10

11

12

13

14

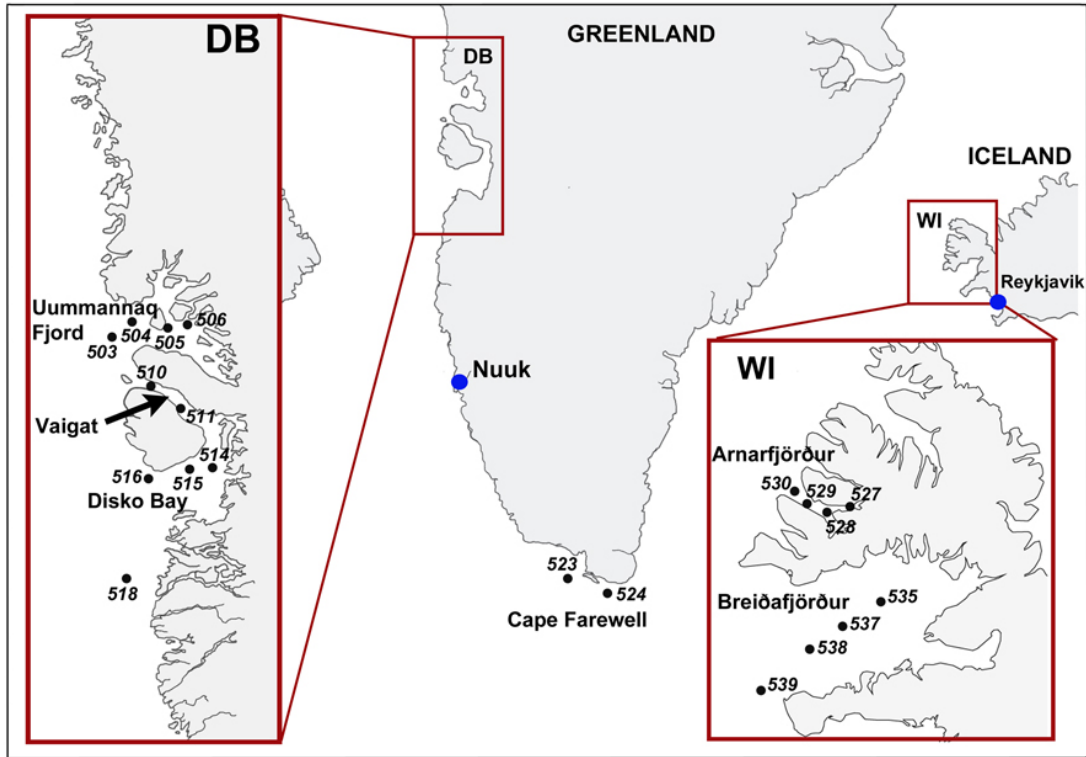
1

2 **FIGURES**

3

4 Fig. 1

5



6

7

8

9

10

11

12

13

14

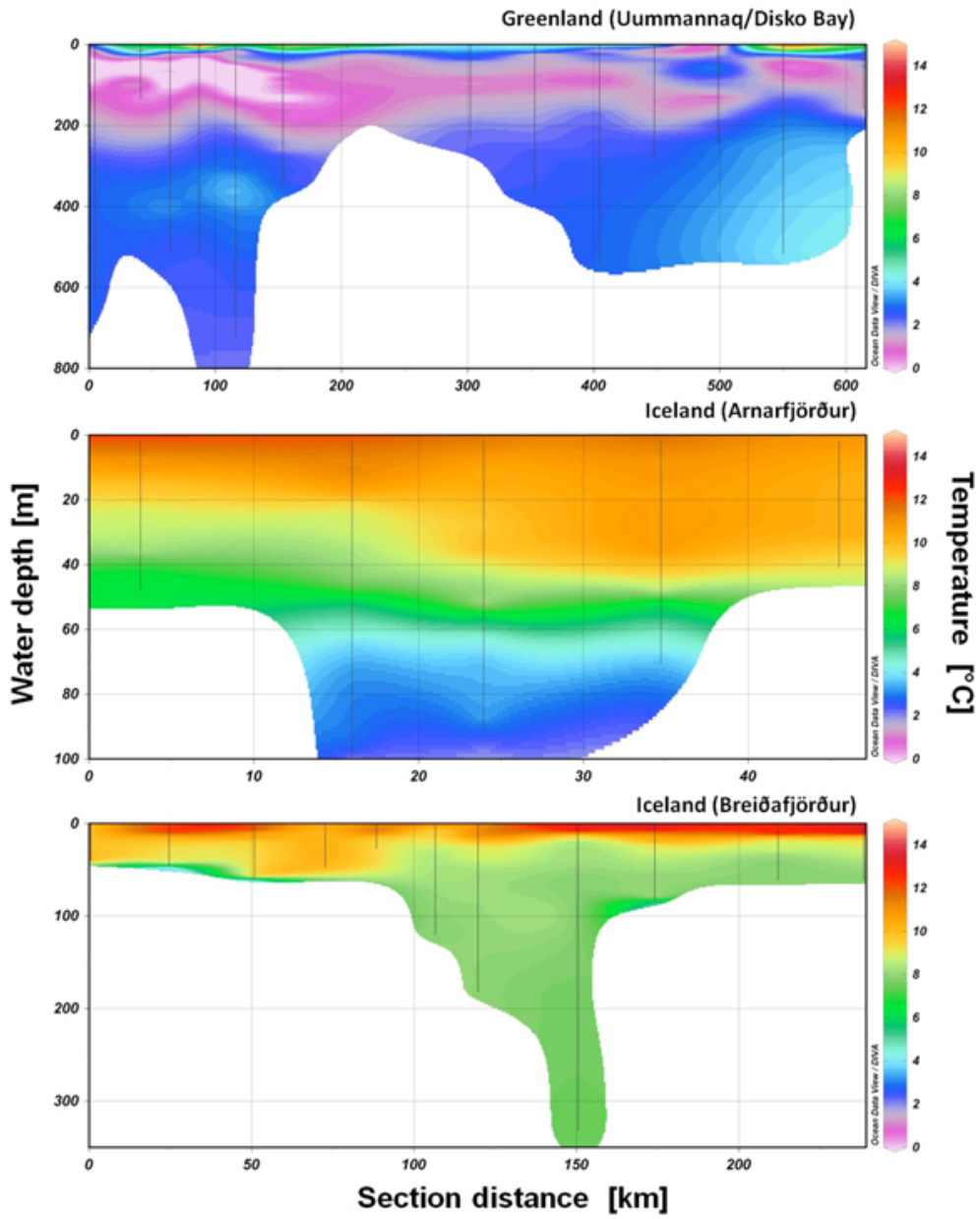
15

1

2

3 Fig. 2

4



5

6

7

8

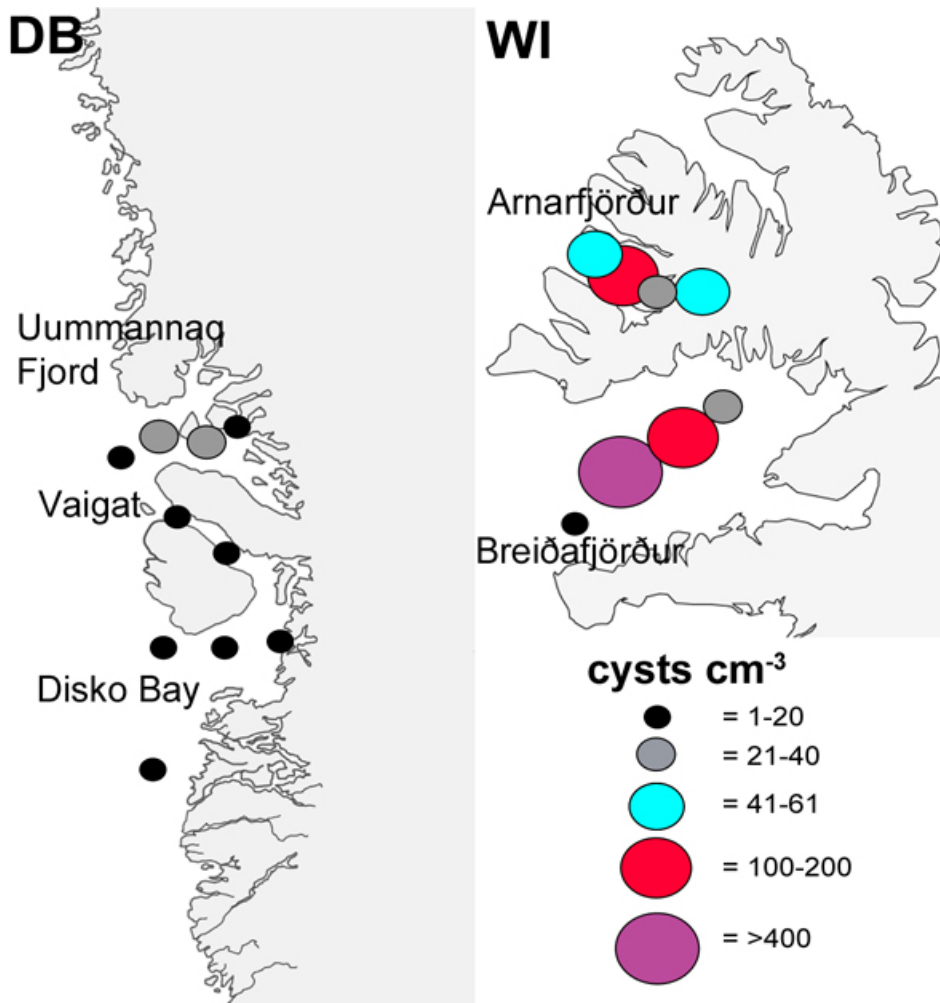
9

1

2

3 Fig. 3

4



5

6

7

8

9

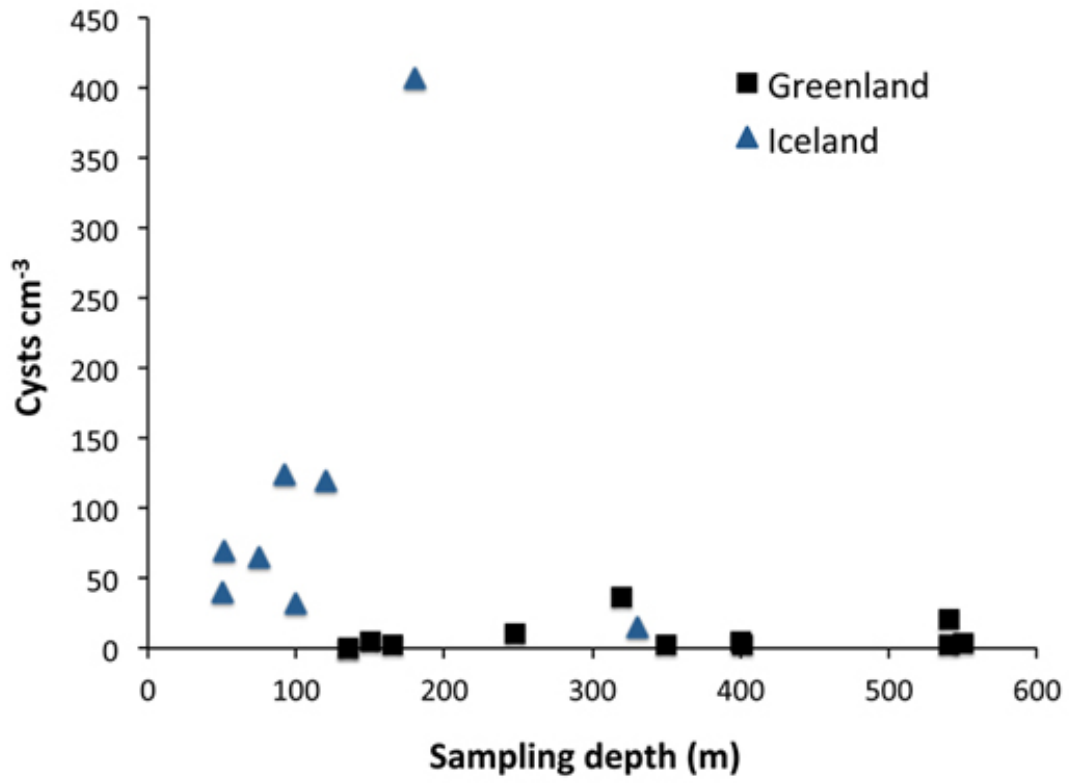
10

11

12

1
2
3
4
5

Fig. 4



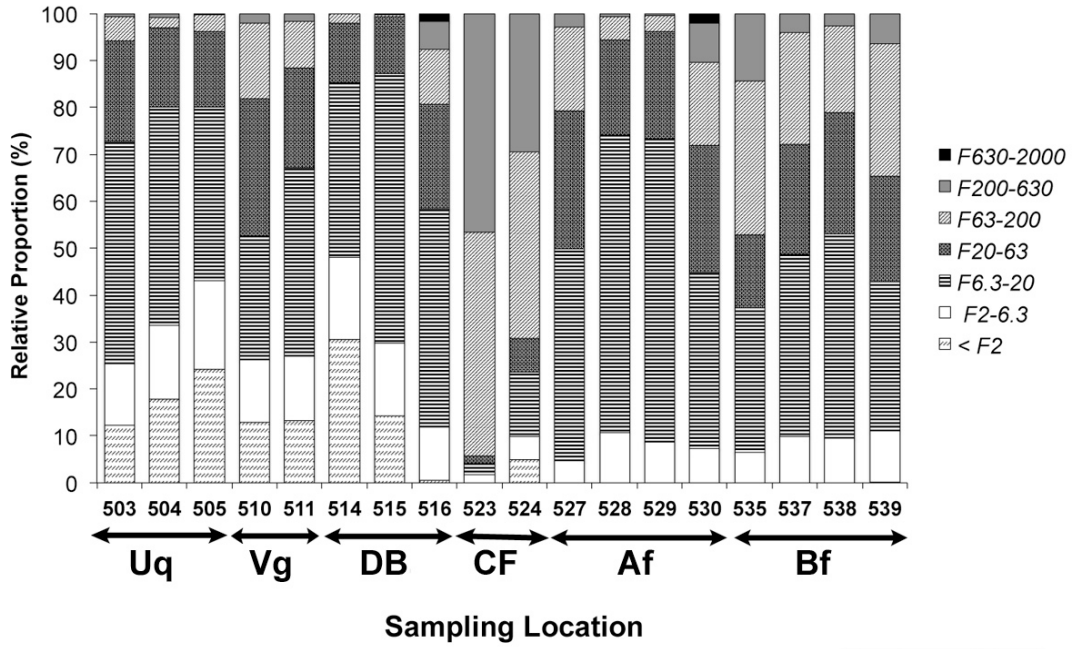
6
7
8
9
10
11
12
13
14
15

1

2

3 Fig. 5

4



5

6

7

8

9

10

11

12

13

14

15

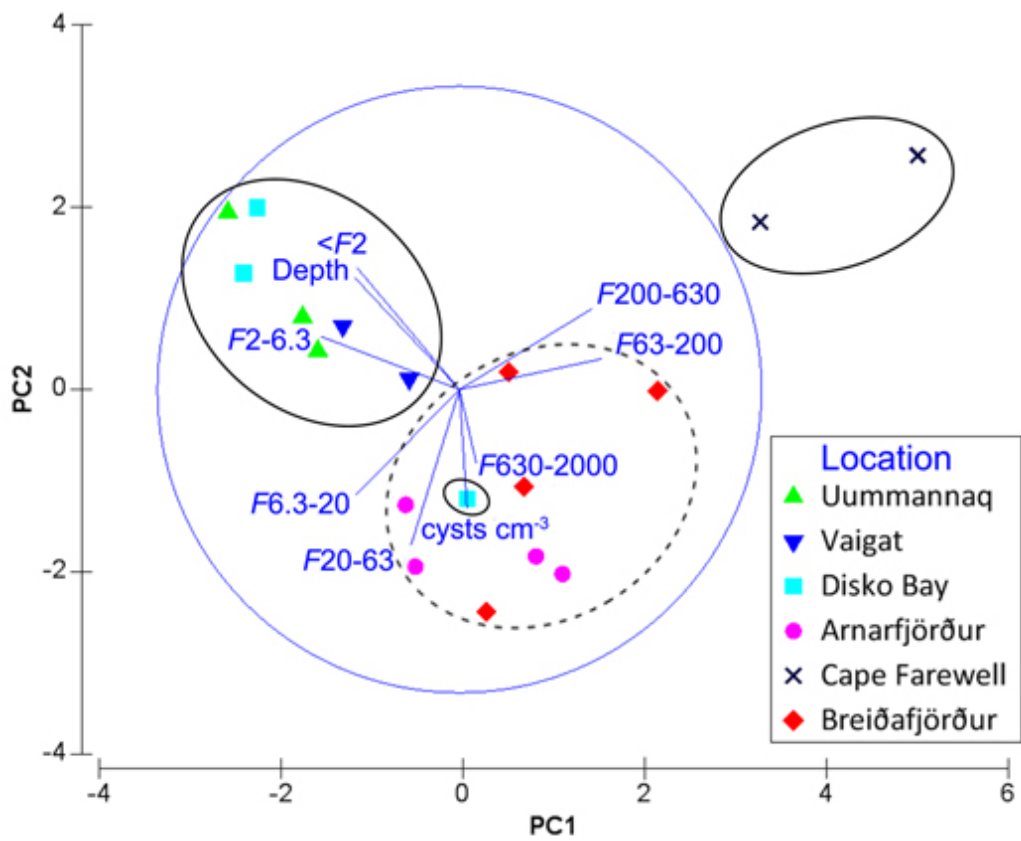
16

17

1

2 Fig. 6

3



4

5

6

7

8

9

10

11

12

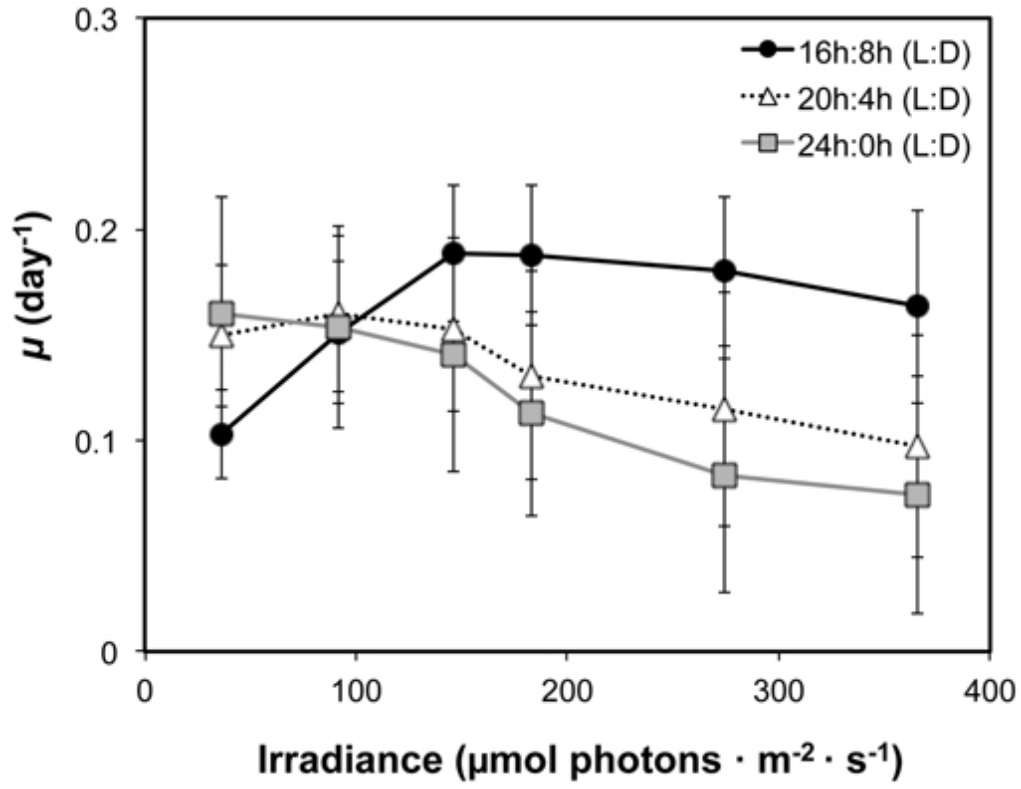
13

14

1

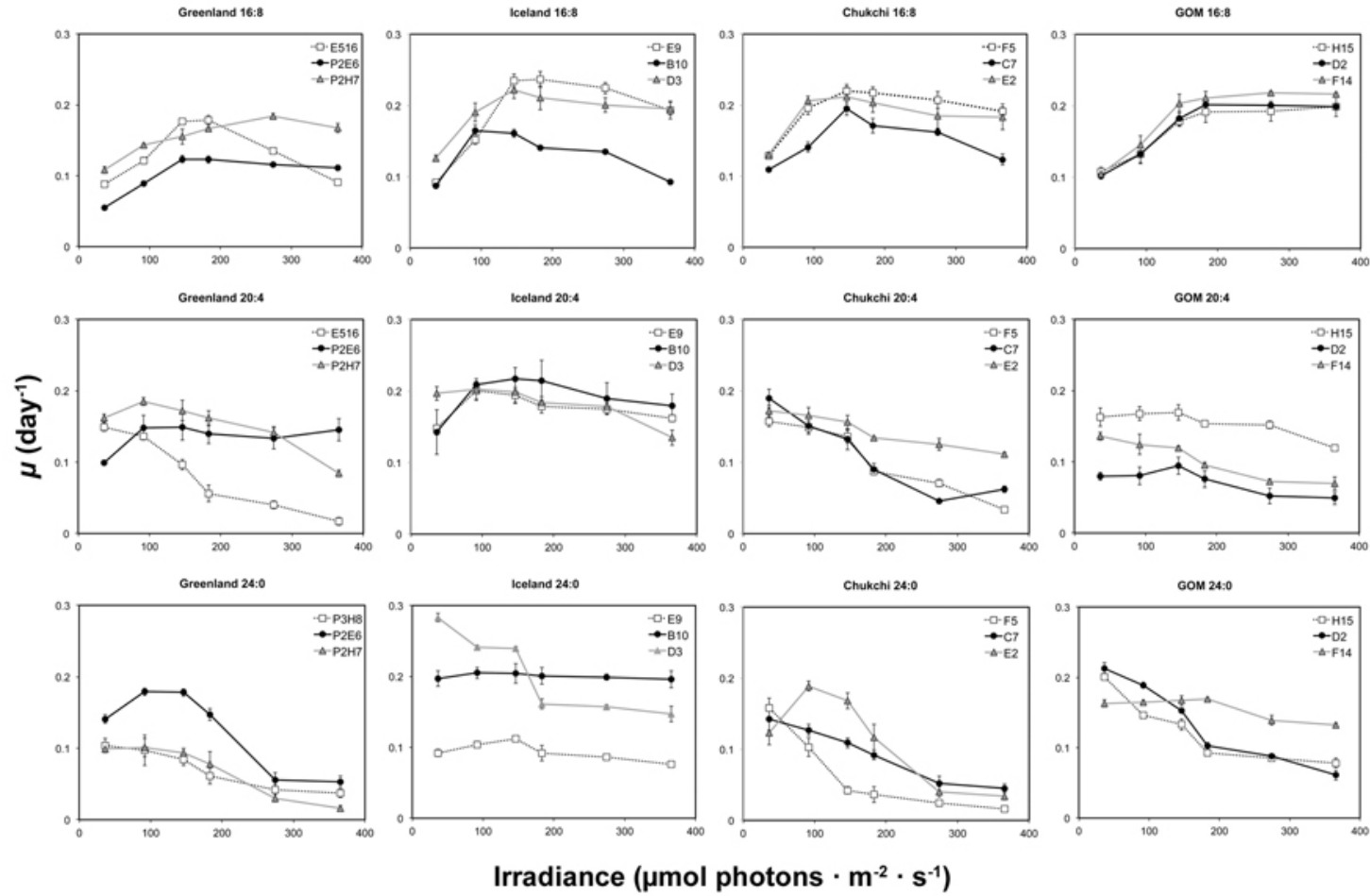
2 Fig. 7

3



4

1 Supplementary Figure S1.



2